

Environmental formation of methylmercury is controlled by synergy of inorganic mercury bioavailability and microbial mercury-methylation capacity

Benjamin D. Peterson ^{1,2}  | David P. Krabbenhoff ³ | Katherine D. McMahon ^{1,4}  | Jacob M. Ogorek ³ | Michael T. Tate ³ | William H. Orem ⁵ | Brett A. Poulin ² 

¹Department of Bacteriology, University of Wisconsin–Madison, Madison, Wisconsin, USA

²Department of Environmental Toxicology, University of California–Davis, Davis, California, USA

³Upper Midwest Water Science Center, Mercury Research Laboratory, U.S. Geological Survey, Madison, Wisconsin, USA

⁴Department of Civil and Environmental Engineering, University of Wisconsin–Madison, Madison, Wisconsin, USA

⁵Geology Energy & Minerals Science Center, U.S. Geological Survey, Reston, Virginia, USA

Correspondence

Benjamin D. Peterson and Brett A. Poulin
Department of Environmental Toxicology,
University of California–Davis, Davis,
California, USA
Email: bdpeterson@ucdavis.edu; bapoulin@ucdavis.edu

Funding information

U.S. National Science Foundation,
Grant/Award Number: CBET-1935173; U.S.
Geological Survey Priority Ecosystems
Science Program; U.S. National Science
Foundation - Graduate Research Fellowships
Program

Abstract

Methylmercury (MeHg) production is controlled by the bioavailability of inorganic divalent mercury (Hg(II)_i) and Hg-methylation capacity of the microbial community (conferred by the *hgcAB* gene cluster). However, the relative importance of these factors and their interaction in the environment remain poorly understood. Here, metagenomic sequencing and a full-factorial MeHg formation experiment were conducted across a wetland sulfate gradient with different microbial communities and pore water chemistries. From this experiment, the relative importance of each factor on MeHg formation was isolated. Hg(II)_i bioavailability correlated with the dissolved organic matter composition, while the microbial Hg-methylation capacity correlated with the abundance of *hgcA* genes. MeHg formation responded synergistically to both factors. Notably, *hgcA* sequences were from diverse taxonomic groups, none of which contained genes for dissimilatory sulfate reduction. This work expands our understanding of the geochemical and microbial constraints on MeHg formation *in situ* and provides an experimental framework for further mechanistic studies.

INTRODUCTION

Methylmercury (MeHg) is the most toxic and bioaccumulative form of mercury (Hg) in the environment (Wiener et al., 2003) and poses significant health risks to humans, fish and wildlife worldwide. MeHg formation by microbes in the environment occurs primarily under low-redox conditions and is dependent on the bioavailability of inorganic divalent Hg (Hg(II)_i) and the Hg-methylating capacity of the microbial community (Hsu-Kim et al., 2013). The geochemical constraints on

Hg(II)_i bioavailability for microbial uptake are controlled by ligand complexation of Hg(II)_i by primarily organic and inorganic reduced S (Graham et al., 2013; Hsu-Kim et al., 2013; Poulin, Gerbig, et al., 2017), whereas Hg(II)_i methylation capacity is conferred by the presence of the *hgcAB* gene cluster (Gilmour et al., 2013; Parks et al., 2013). Previous studies individually investigated the importance of Hg(II)_i bioavailability (Graham et al., 2013; Hsu-Kim et al., 2013; Jonsson et al., 2012) or microbial communities (Christensen et al., 2018; Compeau & Bartha, 1985; Gilmour et al., 1992;

This is an open access article under the terms of the [Creative Commons Attribution](https://creativecommons.org/licenses/by/4.0/) License, which permits use, distribution and reproduction in any medium, provided the original work is properly cited.

© 2023 The Authors. *Environmental Microbiology* published by Applied Microbiology International and John Wiley & Sons Ltd.

Schaefer et al., 2020) to MeHg formation. In amended sediment slurries with simplified ligand chemistries, neither Hg(II)_i bioavailability nor overall microbial activity were strictly limiting; rather, each was shown to influence MeHg production under different conditions (Kucharzyk et al., 2015). In anoxic brackish waters, gene abundance or expression of *hgcA* combined with predicted abundance of Hg(II)_i-sulfide species correlated to MeHg production potentials (Capo, Feng, et al., 2022). A critical step in understanding environmental MeHg production requires the simultaneous quantitative examination of the relative importance of geochemical versus microbial factors to MeHg formation in complex environmental systems, paired with comprehensive measurements of the ligand chemistry and microbial Hg-methylators, which has not yet been done.

Ligand complexation and geochemical speciation of Hg(II)_i ultimately govern Hg(II)_i availability for uptake by microbial cells (Hsu-Kim et al., 2013), which can have long-lasting effects on Hg methylation (Jonsson et al., 2012) and incorporation into the food web (Jonsson et al., 2014). Under environmental conditions lacking inorganic sulfide, Hg(II)_i is exclusively bound to thiol groups (S_{Red}) in dissolved organic matter (DOM) (Haitzer et al., 2002). Conversely, under sulfidic conditions common in anoxic sediments, nano-particulate metacinnabar (β -HgS) dominates Hg(II)_i speciation (Gerbig et al., 2011; Poulin, Gerbig, et al., 2017). The bioavailability of Hg(II)_i associated with nano-particulate β -HgS is greatest at low-to-intermediate sulfide concentrations ($\leq \sim 0.3$ mg/L) and in the presence of DOM of high aromaticity (Graham et al., 2013) and thiol content (Graham et al., 2017). Under very high sulfide concentrations ($> \sim 3$ mg/L), nano-particulate β -HgS becomes crystalline and aggregates (Poulin, Gerbig, et al., 2017), decreasing Hg(II)_i bioavailability for methylation (Zhang et al., 2012). Further, sulfidic conditions enhance the concentration of thiol groups in DOM via sulfurization reactions (Poulin, Ryan, et al., 2017; Vairavamurthy & Mopper, 1987), which enhances the bioavailability of Hg(II)_i to methylation (Bouchet et al., 2018; Graham et al., 2017). However, the net effect of sulfide versus DOM composition and concentration on bioavailability of Hg(II)_i in complex environmental systems is still unclear. In pure culture, efforts to minimize the geochemical complexity of study systems has relied on the use of cysteine as a low-molecular weight analogue to thiols in DOM, which promotes the bioavailability of Hg(II)_i under laboratory conditions (Gilmour et al., 2018; Graham et al., 2012; Schaefer & Morel, 2009). However, the environmental relevance of cysteine controlling the bioavailability of Hg(II)_i has yet to be tested.

The environmental factors controlling the microbial Hg-methylation capacity are poorly understood. Sulfate-reducing bacteria (SRB) have long been

considered a primary microbial guild affiliated with MeHg production due to field experiments under molybdate inhibition (Compeau & Bartha, 1985) or sulfate amendment (Gilmour et al., 1992). However, using the *hgcAB* gene cluster as a molecular marker (Parks et al., 2013), we now recognize the high metabolic and phylogenetic diversity of putative Hg-methylating organisms (Gilmour et al., 2013; Gionfriddo et al., 2016; McDaniel et al., 2020; Podar et al., 2015). Several recent field studies in sulfate-enriched environments observed that SRB accounted for only a small percentage of the *hgcA* abundance, while the majority of *hgcA* abundance was associated with fermentative and syntrophic bacteria or methanogenic archaea (Bae et al., 2014; Jones et al., 2019, 2020; Peterson et al., 2020). Attempts to link *hgcA* abundance to MeHg levels or production have documented mixed results, possibly due to Hg(II)_i bioavailability, limited methodologies, and/or changes in *hgcA* expression/HgcA activity (Bae et al., 2019; Bravo et al., 2016; Capo, Feng, et al. 2022; Christensen et al., 2019; Liu et al., 2018; Millera Ferriz et al., 2021; Roth et al., 2021; Tada et al., 2020). Complex biogeochemical conditions and interdependent microbial communities in the environment also make it difficult to extend observations from laboratory culture studies (Gilmour et al., 2013, 2018; Yu et al., 2018) to natural conditions and anticipate which microbial processes are linked to MeHg production. These complexities may explain the varied response of MeHg production to experimental molybdate inhibition (Bae et al., 2014; Bouchet et al., 2018; Cleckner et al., 1999; Gascón Díez et al., 2016; Schaefer et al., 2020) or sulfate amendment (Gilmour et al., 1992; Jones et al., 2020). Overall, the relationships between microbial community metabolism, *hgcA* gene content and activity, Hg-methylation capacity of the microbial community, and ultimately MeHg production and accumulation are still poorly understood.

To address these knowledge gaps, we quantified the relative importance of Hg(II)_i bioavailability and microbial Hg-methylation capacity on MeHg formation across a sulfate gradient in the Florida Everglades and paired this with microbial community and pore water chemistry characterization. First, a full-factorial MeHg formation experiment was performed using pore waters and intact peat cores collected at six sites across a sulfate gradient to quantify the relative methylation potential of both the pore water and microbial communities in the peat. Next, shotgun metagenomic sequencing was performed to quantify and characterize the microbial community fraction carrying the *hgcA* gene. Together, these complementary approaches facilitated the isolation of geochemical factors governing Hg(II)_i bioavailability from the microbial Hg-methylation capacity (i.e., *hgcA* abundance). Furthermore, genome-resolved metagenomic analyses identified the metabolic potential of microbes with *hgcA* in the peat cores. This study

demonstrates the synergy between geochemical and microbial factors required for environmental MeHg formation, shows that *hgcA* gene abundance is a reliable marker for the Hg-methylation capacity of the microbial community, and provides a valuable experimental framework to target processes underlying MeHg formation in diverse aquatic environments.

EXPERIMENTAL PROCEDURES

Site information and geochemical gradients

The Florida Everglades is an ideal ‘field laboratory’ to study the impact of sulfate concentration and DOM concentration/composition on MeHg production due to the combination of extensive atmospheric Hg deposition (Krabbenhoft et al., 1998; Orem et al., 2020) with long-term geochemical gradients stemming from release points of agricultural run-off (Figure S1) (Orem et al., 2011). In this study, six field sites in Water Conservation Areas 2 (WCA-2) and 3 (WCA-3) and Arthur R. Marshall Loxahatchee National Wildlife Refuge (LOX), were chosen (Table S1; Figure S1) to span a range of sulfate, sulfide, and DOM concentration and

composition (Figure S2). Ambient MeHg concentrations in the peat were lowest in WCA-2, intermediate at the downgradient sites in WCA-3, and highest at 3A-F and LOX8 (Figure 1A). Ambient pore water MeHg concentrations were similarly low at WCA-2, but relatively consistent concentrations were observed across WCA-3 and LOX8 (Figure 1B). Geochemical data and analytical methods are available in Science Base (Tate et al., 2023).

MeHg formation assays

Details for all materials and methods are provided in the Supporting Information. Briefly, at each of the six sites, filtered pore waters and 18 replicate peat cores (7.6 cm diameter) were collected (Figure S1). A suite of water quality and geochemical measurements, including sulfide, sulfate, DOC concentration, and DOM specific ultraviolet absorbance at 254 nm (SUVA₂₅₄), were made on the pore waters using established methods (Figures S2 and S3) (Poulin, Ryan, et al., 2017). Three laboratory-prepared ‘pore waters’ were prepared using purged ultrapure water, all with a background solution matched to the average ionic concentration of Everglades pore water, including 1 mg/L sulfate: ‘F1 HPOA

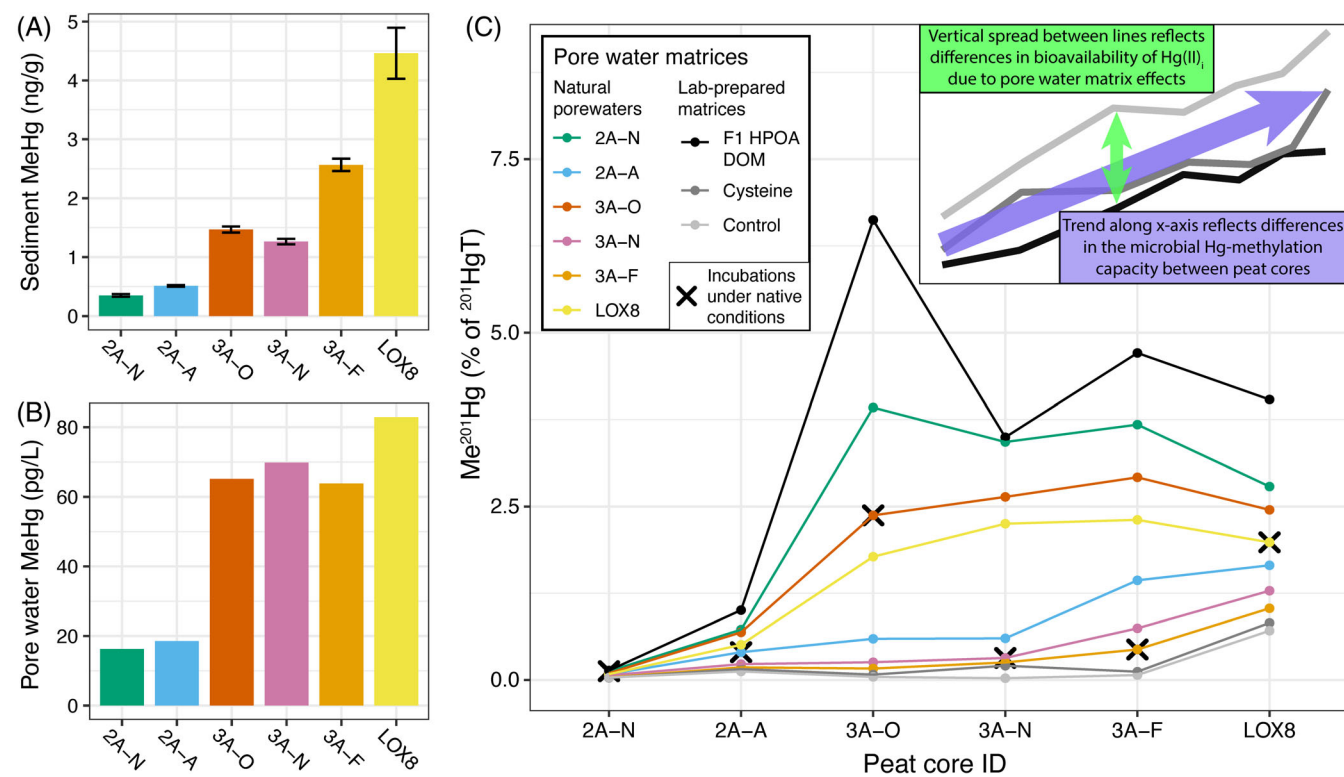


FIGURE 1 Ambient MeHg levels in (A) sediment and (B) pore water, and (C) summary of MeHg formation assay results. Sediment MeHg values represent the average ambient MeHg values across all 18 peat cores from each site. MeHg formation assay results present the mean of duplicate incubations with peat cores and pore waters from the same source. Me ^{201}Hg values are expressed as a percent of the measured ^{201}HgT . Data points marked “X” identify incubations under “native” conditions, where the injected pore water matrices were from the same sites as the peat cores. The inset provides guides for the interpretations of x- and y-axis trends in plot C.

DOM", which contained 90 mg/L of the hydrophobic organic acid fraction (HPOA) of DOM from the F1 site of the Everglades (Poulin, Ryan, et al., 2017); "Cysteine", with 40 μ M of cysteine; and "Control", which had no additional organic ligands. The molar concentration of cysteine matched the concentration of reduced S in the F1 HPOA DOM in pore water solutions (see Supporting Information). The $^{201}\text{Hg(II)}$ tracer was pre-equilibrated with each of the filtered natural and lab-prepared pore waters for a minimum of 4 h. From each of the six field sites, duplicate peat cores were injected with one of the nine different pore water-equilibrated $^{201}\text{Hg(II)}$ tracers in a full-factorial experimental design, for a total of 108 incubations (Figure S4). 1.5 ml of equilibrated tracer was injected every 1 cm from 2 to 10 cm below the top of the core. Injection concentrations were targeted such that the $^{201}\text{Hg(II)}$ amendments to the peat would be 13% of the ambient HgT. After 24 h, the peat cores were frozen to stop the experiment and shipped back to the laboratory on dry ice. The top 2 cm of the core (mostly biofilm) was removed, and the next 4 cm (solid peat) were homogenized for analysis. This was previously shown to be a highly active zone of MeHg production (Gilmour et al., 1998). Excess Me ^{201}Hg was quantified by distillation and isotope dilution with inductively coupled plasma mass spectroscopy (ICP-MS; iCAP, Thermo Scientific) (DeWild et al., 2002; Hintelmann & Evans, 1997), while excess total ^{201}Hg (^{201}HgT) was measured using BrCl oxidation, SnCl₂ reduction, and ICP-MS (Hintelmann & Evans, 1997; Olund et al., 2004). Net Me ^{201}Hg production (NMP) was defined as follows: NMP = excess Me ^{201}Hg /excess $^{201}\text{HgT} \times 100$. Relative methylation potential values were calculated for the pore water (RMP_{matrix}) and the peat cores (RMP_{peat}) by normalizing net Me ^{201}Hg production to the highest net Me ^{201}Hg production value for any incubation using the same peat core or pore water, respectively (Figure S4). A synchronized permutation test using the two-way analysis of variance format (Basso et al., 2009) with log-transformation was done to test for main and interaction effects of the peat core and pore water source on net Me ^{201}Hg production. Model selection was done using Akaike Information Criteria on linear models generated using different combinations of factors. Linear models were used to test for relationships between combinations of RMP_{matrix}, RMP_{peat}, geochemical parameters, and *hgcA* abundance. Incubation data are available in Table S2.

Metagenomics workflow

DNA was isolated from the peat by phenol: chloroform extraction and purified by alcohol precipitation (Lever et al., 2015) then sequenced at QB3 Genomics at the University of California, Berkeley. DNA reads from

duplicate metagenomes were coassembled using both metaSPADEs and MegaHit (Li et al., 2015; Nurk et al., 2017) and open reading frames were predicted from the assembled contigs using Prodigal (Hyatt et al., 2010). HgcA sequences were identified using a custom Hidden Markov Model (Peterson et al., 2020) and manually verified to contain conserved domains (Parks et al., 2013), then dereplicated across assemblies using CD-HIT (Fu et al., 2012). Confirmed HgcA sequences were aligned with the Hg-MATE database (Gionfriddo et al., 2021) and a maximum-likelihood tree was generated using RAxML (Stamatakis, 2014). This, along with a custom workflow (Gionfriddo et al., 2020), was used to assign a taxonomic affiliation to each *hgcA* gene. Normalized abundance of *hgcA* was calculated by first determining the average nucleotide coverage over the *hgcA*-containing contig, then dividing this by the mean coverage of 16 single-copy ribosomal protein genes (Sorek et al., 2007). Thus, the normalized *hgcA* abundance is presented as a percentage of the total microbial community. Genomic bins containing *hgcA* were manually binned using CONCOCT (Alneberg et al., 2014) and refined in Anvi'o (Eren et al., 2015). These bins were taxonomically classified (Chaumeil et al., 2019) and their metabolic pathways identified (Zhou et al., 2022). Raw metagenomic reads are available through the National Center for Biotechnology Information under BioProject accession ID PRJNA808433 and the assemblies, bins and HgcA protein sequences are available through the Open Science Framework (<https://osf.io/8muzf/>). Code for all analyses and figures is stored on Github (<https://github.com/petersonben50/Everglades>).

RESULTS AND DISCUSSION

Net Me ^{201}Hg production in the peat core assays, quantified as the percent of excess ^{201}HgT measured as excess Me ^{201}Hg , ranged from 0% to 8% after 24 h across the six different peat cores incubated with nine pore water matrices ($n = 108$ peat cores total; Figures 1C, S5; Table S2). The inset in Figure 1C shows how the effect of the two variables (peat core vs. pore water matrix source) on net Me ^{201}Hg production can be interpreted in the plot. Across all assays, the response of net Me ^{201}Hg production to the pore water matrix source, visualized as the spread between differently coloured lines in Figure 1C, was consistent regardless of the peat core source (Figures 1C and S6). Changes in net Me ^{201}Hg production in response to the peat core source, visualized as the increase in net Me ^{201}Hg production along the x-axis, were less consistent depending on the pore water matrix, following one of two similar but distinct patterns, discussed in detail below (Figures 1C and S7). Synchronized permutation testing (Basso et al., 2009) showed that both the peat

core source ($p < 0.0001$) and the pore water matrix source ($p < 0.0001$) had significant effects on net Me^{201}Hg production. There was also a statistically significant interaction effect ($p < 0.0001$). This interaction effect is visible in Figure 1C in the two modestly different trends in the peat core effects depending on the source of the pore water matrix (Figures 1C and S7). Four of the pore water matrices (Everglades F1 HPOA, 2A-N, 3A-O, and LOX8) facilitated a dramatic increase in net Me^{201}Hg production in cores from sites 2A-A to 3A-O, but then net Me^{201}Hg production levelled off or modestly decreased in cores from sites across WCA-3A and to LOX8. In contrast, the other five pore water matrices resulted in modest increases in net Me^{201}Hg production in cores from high to low sulfate, with a notable increase in net Me^{201}Hg production in cores from sites 3A-F and LOX8 (Figures 1C and S7). One possible source of this interaction is demethylation activity, which has been shown in isotopically enriched incubations after 8 h in peat from the Everglades and would increase as Me^{201}Hg concentrations increased (Gilmour et al., 1998). Another possibility is the complete methylation of the bioavailable pool of $^{201}\text{Hg}(\text{II})_i$ in the high-producing incubations (Janssen et al., 2016). Either explanation is supported by the observation that pore water matrices that produce the plateau also produced the most Me^{201}Hg and would result in an underestimation of Hg-methylation capacity, particularly at 3A-F and LOX8. Additional possible causes of this interaction effect are discussed in detail in the Supporting Information. Despite this interaction, the relative effects of each pore water matrix and peat core were notably consistent (Figures 1C, S6 and S7). Model selection identified a linear model without the interaction effect as the best fit for the data. Together, this suggests that the independent effects of the peat core and the pore water matrix had a notably larger effect on net Me^{201}Hg production than the interaction between them.

Geochemical controls on $\text{Hg}(\text{II})_i$ methylation

The pore water matrix source had a significant and consistent influence on net Me^{201}Hg production across the six peat cores (Figure 1C and S6), likely by establishing the bioavailability of the $\text{Hg}(\text{II})_i$ tracer, as demonstrated in previous studies (Gilmour et al., 1998; Graham et al., 2012, 2017; Jonsson et al., 2012, 2014; Moreau et al., 2015). Thus, the influence of the pore water matrix on net Me^{201}Hg production reflects changes in $^{201}\text{Hg}(\text{II})_i$ bioavailability due to ligand chemistry (Figure S6). Regardless of the source of the peat core, the Everglades F1 HPOA DOM solution yielded the most bioavailable $^{201}\text{Hg}(\text{II})_i$, which is consistent with previous observations and attributed to the high aromaticity and thiol content of this DOM (Graham

et al., 2013; Moreau et al., 2015; Poulin, Ryan, et al., 2017). Conversely, the control solution always resulted in the lowest net Me^{201}Hg production. Surprisingly, the cysteine solution, which matched the thiol concentration of the Everglades F1 HPOA DOM, also resulted in exceptionally low net Me^{201}Hg production, comparable to the control matrix. The net Me^{201}Hg production of the six natural pore waters were distributed between that of the Everglades F1 HPOA DOM and the control matrix. Those collected from sites closest to where aromatic DOM and sulfate-rich canal water is released to the marshes (Sites 2A-N and 3A-O) consistently promoted the highest net Me^{201}Hg production of the natural pore waters, whereas pore water from sites distant to canal inputs (e.g., sites 2A-A and 3A-F) exhibited notably lower net Me^{201}Hg production levels. LOX8 pore waters resulted in intermediate Me^{201}Hg formation.

To quantify the variation in net Me^{201}Hg production due to pore water matrix source for comparison to geochemical parameters, we calculated a “relative methylation potential” for each of the different pore water matrices ($\text{RMP}_{\text{matrix}}$) as follows. First, incubations were grouped by the source of the peat core; then, net Me^{201}Hg production for each incubation was divided by the highest net Me^{201}Hg production value of any incubation within the group (Figures S4 and S8). Of the measured geochemical properties of the natural and laboratory prepared pore water solutions (DOC, DOM SUVA₂₅₄, inorganic sulfide, UV absorbance), DOM SUVA₂₅₄ exhibited the strongest correlation with $\text{RMP}_{\text{matrix}}$ (adjusted $R^2 = 0.494$; $p < 0.001$; Figure 2).

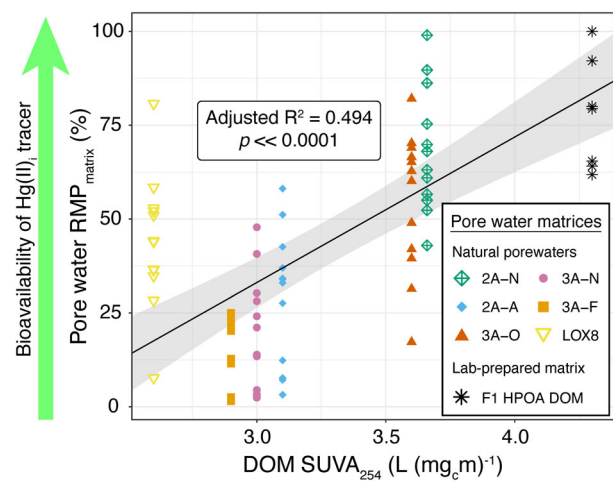


FIGURE 2 Linear correlation between the pore water relative methylation potential ($\text{RMP}_{\text{matrix}}$) and DOM SUVA₂₅₄ of the pore water matrices. The black line represents the linear regression, and the grey shading corresponds to the 98% confidence intervals of the linear fit. The control and cysteine pore water matrices were not included because the solutions do not have SUVA₂₅₄ values. One of the F1 HPOA DOM replicates always resulted in the highest Me^{201}Hg production, so there are six points stacked at $x = 4.3 \text{ L (mg}_c\text{m)}^{-1}$, $y = 100\%$.

Significant correlations with RMP_{matrix} were also observed for DOC concentration (adjusted $R^2 = 0.405$; $p < 0.001$; Figure S9a) and UV_{254} absorbance (adjusted $R^2 = 0.376$; $p < 0.001$; Figure S9b), the latter being a parameter that captures differences in both DOC concentration and DOM aromaticity. This is consistent with extensive prior work showing that high aromatic DOM increases $Hg(II)_i$ bioavailability and facilitates MeHg formation in pure culture experiments (Graham et al., 2012, 2013; Moreau et al., 2015), as more aromatic DOM is not expected to stimulate microbial metabolism in the cores over the short timeframe of the experiments. Sulfide and RMP_{matrix} were positively correlated, albeit weakly (adjusted $R^2 = 0.055$; $p = 0.008$; Figure S9c). While it is known that high sulfide concentrations can inhibit MeHg production (Benoit et al., 1999; Graham et al., 2013) due to the formation of crystalline and aggregated β -HgS of low bioavailability (Poulin, Gerbig, et al., 2017; Zhang et al., 2012), aromatic DOM with high S_{Red} content can inhibit crystalline β -HgS formation and promote $Hg(II)_i$ availability to methylation (Graham et al., 2017; Poulin, Ryan, et al., 2017). We interpret the high pore water RMP_{matrix} from site 2A-N to indicate that even the highest sulfide concentration (3.5 mg/L) was insufficient to suppress $Hg(II)_i$ methylation under the high DOC concentration and high DOM $SUVA_{254}$ (Graham et al., 2013). Sulfate was not correlated to RMP_{matrix} (Figure S9d; $R^2 = 0.026$, $p = 0.051$). We infer that in this system and during the duration of the experiments, the DOM $SUVA_{254}$ is a more important variable than sulfide for controlling $Hg(II)_i$ bioavailability. This is highlighted by the similarity in RMP_{matrix} of 2A-N pore water and F1 HPOA DOM, which were collected from proximal locations, albeit several years apart, and have similar DOC concentrations and DOM $SUVA_{254}$, but very different sulfide concentrations (Figures 2 and S9).

The $Hg(II)_i$ -cysteine solution yielded very low net MeHg formation across all six study sites (Figures 1C and S8) despite having thiol concentration equimolar to the F1 HPOA solution, which is inconsistent with previous pure culture laboratory studies (Graham et al., 2012; Schaefer et al., 2011; Schaefer & Morel, 2009). This is particularly striking considering that cysteine levels in the environment are far lower than those used in this study (Zhang et al., 2004). This may be explained by cysteine's lack of aromaticity needed to sterically inhibit nano-particulate β -HgS growth (Gerbig et al., 2011; Poulin, Gerbig, et al., 2017; Zhang et al., 2012), or the rapid degradation of cysteine under environmental conditions (Chu et al., 2016) that allows the $^{201}Hg(II)_i$ tracer to sorb to the peat, thus diminishing its bioavailability. Regardless of the mechanism, the findings support that cysteine-complexed $Hg(II)_i$ is unlikely to be environmentally relevant for MeHg formation. In total, the results are in general concurrence with laboratory studies demonstrating that

aromatic, thiol-rich DOM plays a key role in promoting $Hg(II)_i$ bioavailability (Graham et al., 2013), with the notable disagreement that cysteine did not promote $Hg(II)_i$ bioavailability in nature.

Microbial controls on $Hg(II)_i$ methylation

The source of the peat cores also had a significant effect on net $Me^{201}Hg$ production. The filtered pore water matrices controlled the bioavailability of the $^{201}Hg(II)_i$ tracer but contained no microbes, whereas the influence of the peat cores on net $Me^{201}Hg$ production reflected the Hg -methylation capacity of the microbial community in the incubation. The net $Me^{201}Hg$ production response to the peat cores was split in one of two similar patterns depending on the pore water matrix used in the incubation, as described above (Figures 1C and S7). However, it was always very low in peat cores from sites with high sulfate and sulfide (2A-N and 2A-A) and increased in peat cores from sites with low to non-detectable sulfate and sulfide.

The relative methylation potential of the peat cores (RMP_{peat}) was quantified to identify the relationship between the Hg -methylation capacity of the microbes and the abundance of the *hgcA* gene. RMP_{peat} was calculated by grouping all incubation assays by the pore water matrix and normalizing net $Me^{201}Hg$ production to the highest level of $Me^{201}Hg$ produced within that group (Figure S4). As observed with the raw net $Me^{201}Hg$ production data (Figure S7), the RMP_{peat} was lowest in peat cores from high sulfate sites (Site 2A-N, 2A-A) and increased systematically in cores with decreasing sulfate (Figure S10). Eighty-seven unique *hgcA* genes across the six sites were identified using shotgun metagenomic sequencing of the peat cores (Tables S3–S5; additional details in Supporting Information). Normalized *hgcA* abundance correlated significantly and positively with RMP_{peat} (adjusted $R^2 = 0.494$; $p < 0.0001$; Figure 3A) due to an increase in *hgcA* abundance from sites with high sulfate to low sulfate (Figure 3B). Previous attempts to correlate *hgcA* abundance to MeHg levels have documented mixed results (Bae et al., 2019; Bravo et al., 2016; Capo, Feng, et al., 2022; Christensen et al., 2019; Liu et al., 2018; Millera Ferriz et al., 2021; Roth et al., 2021; Tada et al., 2020), possibly due to changes in $Hg(II)_i$ bioavailability or methodological constraints of qPCR-based *hgcA* quantification (McDaniel et al., 2020). Other studies suggest additional genes may confer MeHg production (Bowman et al., 2020; Munson et al., 2018). However, the correlation between *hgcA* gene abundance and the microbial Hg -methylation capacity suggests that *hgcA* is the dominant MeHg formation pathway in Everglades peat. Recent work showed decreases in *hgcA* alpha diversity to coincide with decreases in MeHg production thought to be

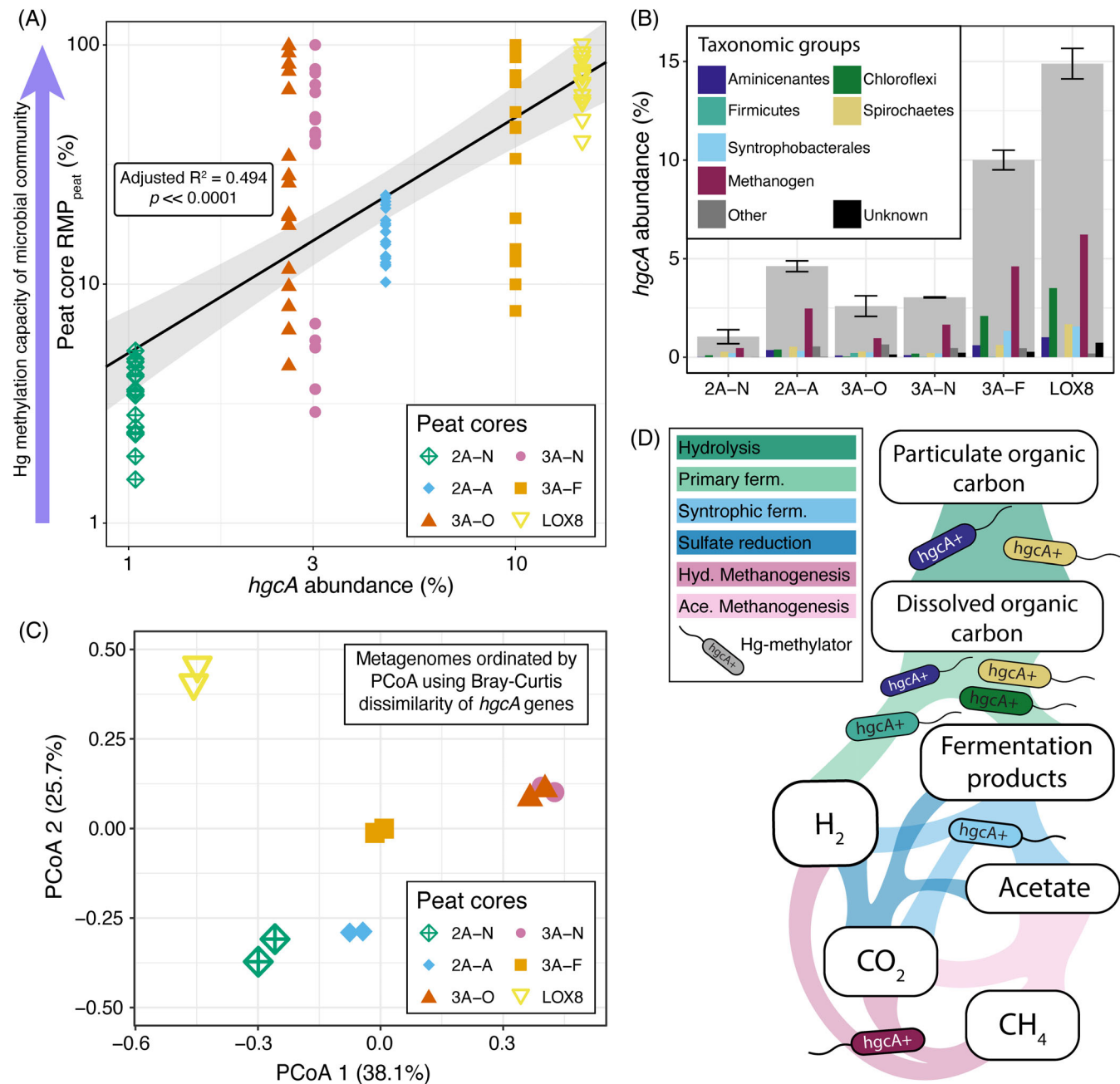


FIGURE 3 Characterization of the microbial community fraction with potential for Hg methylation. (A) The linear correlation between the peat core relative methylation potential (RMP_{peat}) and the normalized $hgcA$ abundance at each site. Both variables were log-transformed before regression. The black line represents the linear regression, and the grey shading corresponds to the 98% confidence intervals of the linear fit. (B) Bar chart of normalized $hgcA$ abundance, with the cumulative abundance of all $hgcA$ sequences shown in grey bars and the abundance of individual taxonomic groups shown in coloured bars. Abundance data are presented as the mean normalized abundance of $hgcA$ in two duplicate metagenomes, with the error bars on the cumulative abundance representing the standard error of duplicates. (C) Principal coordinate analysis (PCoA) of metagenomes based on the Bray–Curtis dissimilarity of the $hgcA$ population in each metagenome. (D) A conceptual model of the anaerobic microbial food web present across the sulfate gradient, with the microbes denoting levels at which organisms with $hgcA$ were identified. Colours of microbes correspond to taxonomic classification in (B). Ace., acetoclastic; Ferm., fermentation; Hyd., hydrogenotrophic.

independent of changes in Hg(II) bioavailability (Jones et al., 2020). This may have reflected an overall decrease in $hgcA$ abundance, as we also observed an increase in $hgcA$ richness and evenness coincident with an increase in $hgcA$ abundance and Hg-methylation capacity (Figure S11). Transcription of

$hgcA$, while thought to be constitutive based on experiments in culture (Gilmour et al., 2011; Goñi-Urriza et al., 2015), varies between different organisms in the environment (Capo, Broman, et al., 2022; McDaniel et al., 2020). Overall trends in $hgcA$ gene abundance versus expression were consistent in brackish waters

(Capo, Feng, et al., 2022), but exhibited divergent trends in sediments from the same site (Capo, Broman, et al., 2022). Collectively, this shows that the controls on *hgcA* gene expression are not well understood. Additionally, the relationship between *hgcA* expression and MeHg production by individual cells is unclear. However, the correlation observed here between *hgcA* and RMP_{peat} suggests that in this ecosystem at least, the *hgcA* abundance, independent of *hgcA* transcription or metabolic activity of the Hg-methylators, is sufficient to identify the Hg-methylation capacity of the microbial community.

Next, the community composition and metabolic potential of the microbes with *hgcA* (*hgcA*+) were evaluated to establish potential linkages between biogeochemical processes and MeHg formation (Table S6). Details of the metabolic analyses are provided in the Supporting Information. The trends in the beta diversity of *hgcA* are not aligned with the trends in the peat core RMP_{peat} or sulfate levels (Figure 3C). Methanogenic archaea-associated *hgcA* genes accounted for the largest portion of *hgcA* abundance (37%–55% of the total *hgcA* coverage; Figures 3B, S12, and S13). These *hgcA* sequences were exclusively associated with predicted hydrogenotrophic or methylotrophic methanogens, but not acetoclastic methanogens, which is consistent with previous work (Gilmour et al., 2018) (Figure 3D). Methanogen-associated *mcrA* genes increased in abundance across the sulfate gradient (Figure S14a). A comparison of methanogen-associated *hgcA* and *mcrA* abundances indicates that 50%–100% of methanogens across the sulfate gradient carried *hgcA* (Figures 3B and S14a). The remainder of the *hgcA* sequences were from a diverse group of *hgcA*+ bacteria, including Chloroflexi, Aminicenantes, Spirochaetes, and non-SRB Syntrophobacterales, among other rarer groups (Table S5). Metabolic pathway analysis of reconstructed *hgcA*+ genomes from Chloroflexi, Aminicenantes, and Syntrophobacterales and comparison of unbinned *hgcA* to genomes with closely related genes confirmed that all classified non-methanogen-associated *hgcA*+ microbes in these peat cores are fermentative (Figure 3D). Several *hgcA* genes were highly divergent from the *hgcA* sequences in the reference database, resulting in 0%–5% of the *hgcA* genes (by abundance) being unclassified with no information on the metabolic potential. Importantly, none of the *hgcA* sequences were expected to be associated with SRB (Figure 3D). This is not due to a lack of SRB, as SRB accounted for up to 4.5% or 7.5% (depending on the marker used) of the microbial population, increasing in abundance across the sulfate gradient (Figure S14b). This surprising finding is discussed in detail below. Although subtle differences in the taxonomic affiliation of *hgcA*+ community members were observed across the six sites, the relative contribution of organisms from different levels of the microbial food

web to the *hgcA* pool do not differ substantially with respect to sulfate levels (Figures 3D and S13). Thus, we hypothesize that the metabolic pathways directly contributing to MeHg production are likely consistent across the sulfate gradient. This consistency and the linear relationship between RMP_{peat} and overall *hgcA* abundance (Figure 3A) suggest that the observed differences in the Hg-methylation capacity are governed by abundance of Hg-methylators rather than their metabolic activity.

While recent studies have shown SRB to account for a small percentage of the microbial community even under sulfidic conditions (Capo, Broman, et al., 2022; Jones et al., 2019, 2020; Peterson et al., 2020), including within the greater Everglades ecosystem (Bae et al., 2014), none of these have confirmed the absence of SRB-associated *hgcA* sequences. Molybdate inhibition experiments have shown the importance of sulfate reduction for MeHg production in Everglades peat, particularly in the high sulfide sites (Bae et al., 2014; Gilmour et al., 1998). Together, this suggests that SRB play an indirect role in MeHg production in the peat that is not represented by the abundance of SRB-associated *hgcA* genes. It is possible that rare *hgcA*-carrying SRB, undetected due to insufficient sequencing depth, influenced MeHg formation; however, this is unlikely given the complete absence of SRB-associated *hgcA* sequences and the close linear relationship between *hgcA* and MeHg production capacity (Figure 3A). Alternatively, SRB could indirectly control MeHg formation by controlling carbon and energy flow, both above (fermentation) and below (methanogenesis), through the anaerobic microbial food web, thus influencing the metabolic activity of *hgcA*+ organisms in the community. For example, under anoxic conditions, fermentative organisms break down and convert large organic molecules into smaller carbon compounds, but they rely on syntrophs or respiratory organisms to consume these products (Figure 3D) (Arndt et al., 2013). SRB can oxidize smaller organic molecules either by reducing sulfate or in syntrophy with methanogens, where they ferment volatile fatty acids (e.g., propionate, butyrate) to methanogenic substrates (acetate, CO₂ and hydrogen) (Sieber et al., 2012). The parallel increase in *mcrA* and *dsrAD* with decreasing sulfide levels may indicate increasing levels of SRB-methanogenic syntrophy (Figure S14). These syntrophic interactions are known to enhance MeHg formation (Yu et al., 2018), and given the high *hgcA* abundance within the methanogenic community, may contribute to the observed increase in Hg-methylation capacity (Figure S10). If *hgcA*-containing methanogens are reliant on SRB through syntrophy, this could explain the inhibition of MeHg formation by molybdate as well (Bae et al., 2014; Cleckner et al., 1999; Gilmour et al., 1998; Newport & Nedwell, 1988). Overall, we hypothesize that terminal

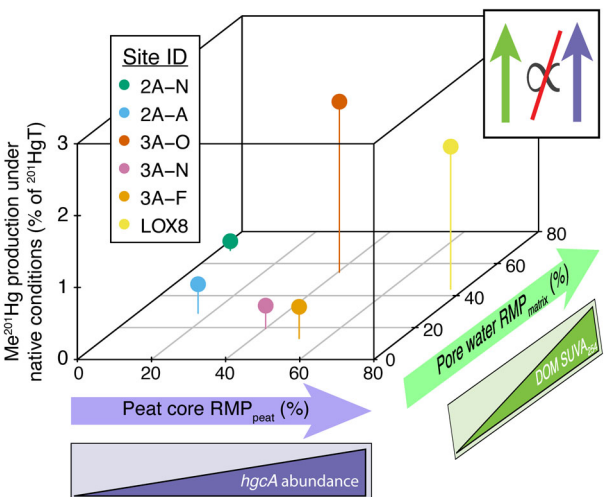


FIGURE 4 Effects of Hg(II), bioavailability and Hg-methylation capacity of microbial community on the production of MeHg under “native” conditions. Native MeHg production is based on MeHg formation assay results using peat cores injected with ^{201}Hg (II), equilibrated with pore water from the same site. Native MeHg production data are presented as the percent of ^{201}HgT measured as Me^{201}Hg . Environmental parameters that were observed to influence the bioavailability of Hg(II)_i and the microbial Hg-methylation capacity are shown below the respective axes. Inset shows there is no correlation between RMP_{matrix} and RMP_{peat} ($p = 0.32$).

respiration is dominated by sulfate reduction and hydrogenotrophic methanogenesis at sulfate-enriched sites, whereas low sulfate sites exhibit greater fermentation of small organic acids by SRB coupled syntrophically to hydrogenotrophic methanogenesis and acetate consumption by acetoclastic methanogens.

MeHg production and accumulation

A major knowledge gap in the field is whether Hg(II)_i bioavailability or Hg-methylation capacity is the rate-limiting step for MeHg production in environmental systems. By isolating these two effects, we were able to compare them to each other and to the production of MeHg. There was no correlation between Hg(II)_i bioavailability (RMP_{matrix}) and Hg-methylation capacity (RMP_{peat}; Figure 4), suggesting that the ability of microbial communities to methylate Hg was not linked to how much bioavailable Hg was present. This supports the hypothesis that MeHg production is not the “native function” of *hgcA*, as has been proposed in previous work (Parks et al., 2013; Smith et al., 2015). We also compared how each factor influenced MeHg production under *in situ* conditions, termed “native MeHg production”. Neither factor was solely limiting for native MeHg production; rather, a synergy of the two factors was required. Native MeHg production was only high at sites where both the pore water RMP_{matrix} and the

microbial community RMP_{peat} were high (Figure 4). For example, peat from sites 3A-O and 3A-N had similar *hgcA*⁺ microbial communities (Figure 3B,C) that also corresponded to nearly identical RMP_{peat} values (Figure 3A). However, native MeHg production at site 3A-O was much higher due to higher RMP_{matrix} values (Figure 4), which are linked to the higher DOM SUVA₂₅₄ promoting Hg(II)_i bioavailability (Figure 2). Conversely, the pore water RMP_{matrix} at site 2A-N was similar to that at site 3A-O, but the low RMP_{peat} at 2A-N was responsible for the very low native MeHg production (Figure 4). This synergistic effect is consistent with work in brackish marine waters that showed predicted concentrations of Hg(II)-sulfide complexes and gene abundance or expression of *hgcA* collectively correlated with MeHg production potential (Capo, Feng, et al., 2022). Together, these data suggest that Hg(II)_i bioavailability and the Hg-methylation capacity of the microbial community both control MeHg formation under environmental conditions and that either of them can limit MeHg production (Figure 5).

Another major knowledge gap is how MeHg production and the factors that govern it relate to ambient MeHg pools in sediment and pore water which have accumulated over time. In this study, MeHg concentrations in the peat (Figure 1A) and pore water (Figure 1B) increased systematically with decreasing sulfate. However, the pattern in Me^{201}Hg formation under native conditions was much different, showing high net Hg formation rates at 3A-O and LOX8, but low at the other four sites (Figure 1C). Additionally, we observed MeHg production up to 3.4% of the tracer under ambient conditions at 3A-O but the %MeHg values at this site are only 1.5%. These observations may be due, in part, to other biogeochemical processes influencing ambient MeHg levels that were not measured in this study. One likely possibility is that much of the ambient Hg(II)_i is sorbed strongly to the peat and is not available for methylation, but it is unclear how this would change across the sulfate gradient. Another likely process is MeHg degradation, which does occur in Everglades peat (Gilmour et al., 1998; Marvin-DiPasquale & Oremland, 1998). The demethylation gene *merB* was detected at all sites and decreased in abundance with decreasing sulfate concentrations, in opposition to the trend in *hgcA* (Figure S15); however, demethylation occurs at a consistent rate across the sulfate gradient in Everglades peat (Marvin-DiPasquale & Oremland, 1998). Despite these other potential effects, calculated RMP_{peat} values and ambient MeHg concentration in the peat were strongly and positively correlated (adjusted $R^2 = 0.885$; $p = 0.003$; Figure S16a), while RMP_{matrix} values were not correlated with ambient MeHg concentration in the peat (adjusted $R^2 = -0.250$; $p = 0.9759$; Figure S16b). We propose that RMP_{peat} represents the longer-term, site-specific MeHg production potential, whereas RMP_{matrix}

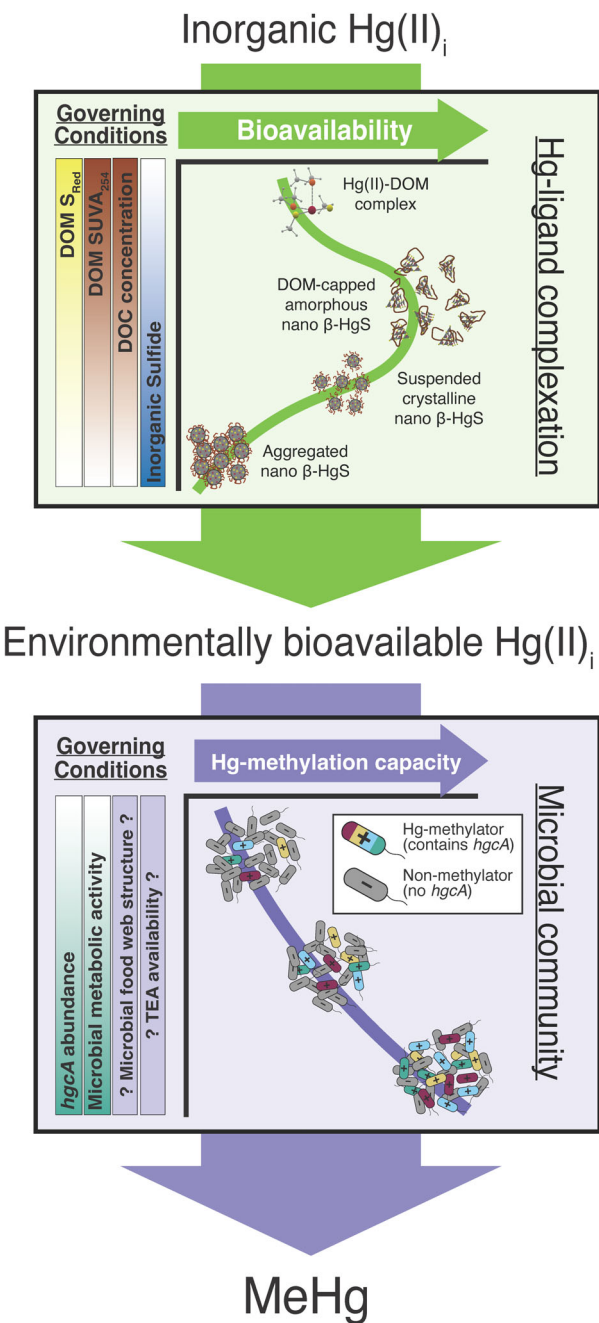


FIGURE 5 Conceptual model of MeHg production as a two-step process: first, the formation of bioavailable Hg(II)_i, followed by microbial methylation of bioavailable Hg(II)_i. Environmental MeHg formation is limited by both factors, which in turn have several environmental drivers. The roles of DOM quantity and composition and sulfide in regulating bioavailable Hg(II)_i in the environment is informed by results of this study and others on Hg(II)_i complexation (Haitzer et al., 2002; Manceau et al., 2015), nanoparticulate β -HgS formation (Gerbig et al., 2011; Poulin, Gerbig, et al., 2017) and Hg(II)_i bioavailability to methylation (Graham et al., 2012, 2013, 2017; Zhang et al., 2012). The relationship between hgcA abundance and Hg-methylation capacity of a microbial community is informed by results of this study and others on hgcA-based Hg methylation (Gilmour et al., 2013; Parks et al., 2013) and Hg-methylation correlations with overall microbial activity (Guimarães et al., 2006). While many studies have identified Hg methylators across the anaerobic microbial food web (Gilmour et al., 2013; Gionfriddo et al., 2016; Jones et al., 2019; McDaniel et al., 2020; Peterson et al., 2020), it is still unknown how the distribution of hgcA across these metabolic guilds or their response to changing terminal electron acceptors (TEAs) influences MeHg production.

represents the potential shorter-term (seasonal) effects of aqueous ligands promoting Hg(II)_i methylation.

Role of sulfate in controlling MeHg production in the environment

This study offers new insights into the long-standing hypothesis that sulfate and sulfide are the master variables controlling MeHg production and add complexity to the well-documented linkages between anthropogenic sulfate loading and MeHg production across the Everglades (Gilmour et al., 1998; Hurley et al., 1998; Orem et al., 2020) and other peatlands worldwide (Coleman Wasik et al., 2012, 2015; Mitchell et al., 2008; Poulin et al., 2019; Tjerngren et al., 2012). The current model is that at high sulfide concentrations, Hg(II)_i bioavailability is drastically reduced, due to the formation of crystalline nano-particulate β -HgS of lower bioavailability (Gerbig et al., 2011; Gilmour et al., 2018; Poulin, Gerbig, et al., 2017; Zhang et al., 2012), while low sulfate concentrations result in lowered SRB activity, leading to reduced MeHg production. Collectively, this was used to explain the “Goldilocks curve” observed in the Everglades, where MeHg formation is maximum under intermediate sulfate and sulfide concentrations (Gilmour et al., 2007; Orem et al., 2020). However, we showed that the low MeHg production at high sulfate sites was due to reduced Hg-methylation capacity by the microbial community, despite the Hg(II)_i bioavailability being high. For example, 2A-N pore water resulted in high MeHg production when paired with cores containing high hgcA abundance, but hgcA at 2A-N was low, resulting in low MeHg production under native conditions (Figures 1C and 3B). At the low sulfate end of the gradient, microbial Hg-methylation capacity was highest (high hgcA abundance), but the low bioavailability of Hg(II)_i led to reduced MeHg production levels. For example, the peat cores from 3A-F produced high MeHg when provided with ²⁰¹Hg(II)_i equilibrated with pore water from 2A-N, LOX8, or F1 HPOA DOM due to the high hgcA content at 3A-F, but the low bioavailability of ²⁰¹Hg(II)_i in 3A-F pore water drove low MeHg production under native conditions (Figure 1C).

Thus, the influence of anthropogenic sulfate levels on the overall redox status of wetlands and SRB activity on Hg methylation in the Florida Everglades and similarly impacted wetlands is more complicated than previously described. Sulfate reduction exerts control on Hg(II)_i bioavailability in a number of ways. While sulfide can precipitate Hg(II)_i (Poulin, Gerbig, et al., 2017), reducing its overall bioavailability, this is unlikely to be a dominant process in sites with high concentrations of aromatic DOM, given the high Hg(II)_i bioavailability at the high sulfide sites (Figure S8). On the other hand, moderate levels of sulfide, in the presence of aromatic DOM, can enhance methylation by promoting the

formation of poorly crystalline nano-particulate β -HgS (Gerbig et al., 2011; Poulin, Gerbig, et al., 2017). Enhanced sulfate reduction can also promote peat degradation, increasing the concentration of high-SUVA₂₅₄ DOM (Aiken et al., 2011; Luek et al., 2017) and DOM S_{Red} content via sulfurization (Poulin, Ryan, et al., 2017) in wetland pore waters; both of these enhance the bioavailability of Hg(II)_i to methylation (Graham et al., 2012, 2013, 2017; Jonsson et al., 2012; Zhang et al., 2012). The effects of sulfate loading on the Hg-methylating microbial community are less clear. Overall, both *hgcA* abundance and RMP_{peat} decreased with higher overall sulfate concentrations (Figures 3B and S10), consistent with the lack of *hgcA+* SRB and previous work showing a decrease in *hgcA* diversity and estimated Hg-methylation capacity with increased long-term sulfate loading (Jones et al., 2020). However, past work has clearly shown that SRB activity is important for MeHg production in the Everglades (Bae et al., 2014; Gilmour et al., 1998; Orem et al., 2020). Thus, we propose that SRB influence MeHg production indirectly by stimulating overall microbial metabolism, possibly through consuming fermentation products (Arndt et al., 2013) and/or by stimulating methanogenic activity through syntrophy (Sieber et al., 2012). Ultimately, functional assays and the deployment of next-generation physiology experiments (Hatzenpichler, 2020) are needed to further probe how the metabolic activity and interactions of the microbial community influence MeHg production.

CONCLUSIONS AND ENVIRONMENTAL IMPLICATIONS

This study presents a dual examination of microbial and geochemical controls on MeHg production in natural peatlands, providing new insights into both the synergy between the *hgcA+* fraction of the microbial community and geochemical controls on Hg(II)_i bioavailability, and the direct and indirect roles of sulfate. The abundance of metabolically diverse populations with *hgcA* confer robust potential for Hg-methylation; when paired with geochemical conditions that promote Hg(II)_i bioavailability, one can expect MeHg formation and a high potential for food web uptake and MeHg biomagnification to toxic levels. Given the widely recognized importance of sulfate on spatial and temporal trends in MeHg formation in wetlands globally (Coleman Wasik et al., 2012, 2015; Mitchell et al., 2008; Orem et al., 2020; Poulin et al., 2019; Tjerngren et al., 2012), a mechanistic understanding of the role of sulfate loading on MeHg production is critical. Peatland ecosystems are experiencing seasonal and long-term increases in sulfate levels in response to increased sulfate use in agricultural practices (Hinckley et al., 2020) and coastal wetland inundation with

seawater sulfate (Chambers et al., 2019). The results here suggest that ecosystems with lower sulfate levels but high DOM concentration and SUVA₂₅₄ quality may be well-poised to form MeHg when sulfate levels increase due to the indirect effects of sulfate on Hg(II)_i bioavailability. We postulate that the bioavailability of Hg(II)_i in environments with lower DOC levels (e.g., marine waters) may be modulated by inorganic sulfide in addition to DOM (Capo, Feng, et al. 2022). We still have much to learn on how environmental conditions such as sulfate concentrations influence *hgcA* distribution and how interactions between different metabolic guilds influence overall MeHg formation rates. Notwithstanding, this study provides an important framework by which the individual factors that influence MeHg production can be isolated and highlights the need for more advanced methods to elucidate the mechanism by which these factors drive MeHg formation.

AUTHOR CONTRIBUTIONS

Benjamin D. Peterson: Conceptualization (equal); data curation (equal); formal analysis (lead); investigation (equal); methodology (equal); validation (equal); visualization (lead); writing – original draft (lead); writing – review and editing (lead). **David P. Krabbenhoft:** Conceptualization (lead); data curation (lead); formal analysis (equal); funding acquisition (lead); investigation (equal); methodology (lead); resources (equal); supervision (equal); validation (equal); writing – original draft (equal); writing – review and editing (equal). **Katherine D. McMahon:** Conceptualization (equal); formal analysis (equal); funding acquisition (equal); methodology (equal); resources (equal); supervision (equal); visualization (supporting); writing – original draft (supporting); writing – review and editing (supporting). **Jacob M. Ogorek:** Data curation (equal); formal analysis (equal); methodology (equal); resources (equal); supervision (equal); validation (equal). **Michael T. Tate:** Data curation (equal); formal analysis (equal); investigation (equal); methodology (equal); validation (equal). **William H. Orem:** Funding acquisition (supporting); investigation (supporting); methodology (supporting); resources (supporting); writing – review and editing (supporting). **Brett A. Poulin:** Conceptualization (equal); data curation (lead); formal analysis (equal); funding acquisition (equal); investigation (equal); methodology (equal); project administration (lead); resources (equal); supervision (lead); validation (equal); visualization (equal); writing – original draft (equal); writing – review and editing (equal).

ACKNOWLEDGEMENTS

This work was supported by the U.S. Geological Survey (USGS) Priority Ecosystems Science (PES) program (support to David P. Krabbenhoft and Brett A. Poulin). Katherine D. McMahon and Benjamin

D. Peterson were supported by a grant from the U.S. National Science Foundation (CBET-1935173). Benjamin D. Peterson was supported by the U.S. National Science Foundation Graduate Research Fellowship Program. All mercury analyses were performed at the Upper Midwest Water Science Center in the Mercury Research Laboratory (U.S. Geological Survey, Madison, WI). Computational analyses were done on the Wisconsin Energy Institute computing cluster, which is funded by the Great Lakes Bioenergy Research Center as part of the U.S. Department of Energy Office of Science. Any use of trade, product or firm names in this publication is for descriptive purposes only and does not imply endorsement by the U.S. Government.

CONFLICT OF INTEREST

The authors declare no conflicts of interest.

DATA AVAILABILITY STATEMENT

All metagenomic, incubation and geochemical data are available as supplemental data or online, as outlined in the methods section.

ORCID

Benjamin D. Peterson  <https://orcid.org/0000-0001-5290-9142>

Katherine D. McMahon  <https://orcid.org/0000-0002-7038-026X>

Brett A. Poulin  <https://orcid.org/0000-0002-5555-7733>

REFERENCES

Aiken, G.R., Gilmour, C.C., Krabbenhoft, D.P. & Orem, W.H. (2011) Dissolved organic matter in the Florida Everglades: implications for ecosystem restoration. *Critical Reviews in Environmental Science and Technology*, 41(S1), 217–248. Available from: <https://doi.org/10.1080/10643389.2010.530934>

Alneberg, J., Bjarnason, B.S., de Brujin, I., Schirmer, M., Quick, J., Ijaz, U.Z. et al. (2014) Binning metagenomic contigs by coverage and composition. *Nature Methods*, 11(11), 1144–1146. Available from: <https://doi.org/10.1038/nmeth.3103>

Arndt, S., Jørgensen, B.B., LaRowe, D.E., Middelburg, J.J., Pancost, R.D. & Regnier, P. (2013) Quantifying the degradation of organic matter in marine sediments: a review and synthesis. *Earth-Science Reviews*, 123, 53–86. Available from: <https://doi.org/10.1016/j.earscirev.2013.02.008>

Bae, H.-S., Dierberg, F.E. & Ogram, A. (2014) Syntrophs dominate sequences associated with the mercury methylation-related gene *hgcA* in the water conservation areas of the Florida Everglades. *Applied and Environmental Microbiology*, 80(20), 6517–6526. Available from: <https://doi.org/10.1128/AEM.01666-14>

Bae, H.-S., Dierberg, F.E. & Ogram, A. (2019) Periphyton and flocculent materials are important ecological compartments supporting abundant and diverse mercury methylator assemblages in the Florida Everglades. *Applied and Environmental Microbiology*, 85(13), 1–17. Available from: <https://doi.org/10.1128/AEM.00156-19>

Basso, D., Pesarin, F., Salmaso, L. & Solari, A. (2009) *Permutation tests for stochastic ordering and ANOVA: theory and applications with R*. New York, NY: Springer.

Benoit, J.M., Gilmour, C.C., Mason, R.P. & Heyes, A. (1999) Sulfide controls on mercury speciation and bioavailability to methylating bacteria in sediment pore waters. *Environmental Science & Technology*, 33(6), 951–957. Available from: <https://doi.org/10.1021/es9808200>

Bouchet, S., Goñi-Urriza, M., Monperrus, M., Guyoneaud, R., Fernandez, P., Heredia, C. et al. (2018) Linking microbial activities and low-molecular-weight thiols to Hg methylation in biofilms and periphyton from high-altitude tropical lakes in the Bolivian altiplano. *Environmental Science & Technology*, 52(17), 9758–9767. Available from: <https://doi.org/10.1021/acs.est.8b01885>

Bowman, K.L., Collins, R.E., Agather, A.M., Lamborg, C.H., Hammerschmidt, C.R., Kaul, D. et al. (2020) Distribution of mercury-cycling genes in the Arctic and equatorial Pacific oceans and their relationship to mercury speciation. *Limnology and Oceanography*, 65, S310–S320. Available from: <https://doi.org/10.1002/lno.11310>

Bravo, A.G., Loizeau, J.-L., Dranguet, P., Makri, S., Björn, E., Ungureanu, V.G. et al. (2016) Persistent Hg contamination and occurrence of Hg-methylating transcript (*hgcA*) downstream of a chlor-alkali plant in the Olt River (Romania). *Environmental Science and Pollution Research*, 23(11), 10529–10541. Available from: <https://doi.org/10.1007/s11356-015-5906-4>

Capo, E., Broman, E., Bonaglia, S., Bravo, A.G., Bertilsson, S., Soerensen, A.L. et al. (2022) Oxygen-deficient water zones in the Baltic Sea promote uncharacterized Hg methylating microorganisms in underlying sediments. *Limnology and Oceanography*, 67, 135–146. Available from: <https://doi.org/10.1002/lno.11981>

Capo, E., Feng, C., Bravo, A.G., Bertilsson, S., Soerensen, A.L., Pinhassi, J. et al. (2022) Expression levels of *hgcAB* genes and mercury availability jointly explain methylmercury formation in stratified brackish waters. *Environmental Science & Technology*, 56(18), 13119–13130. Available from: <https://doi.org/10.1021/acs.est.2c03784>

Chambers, L.G., Steinmuller, H.E. & Breithaupt, J.L. (2019) Toward a mechanistic understanding of “peat collapse” and its potential contribution to coastal wetland loss. *Ecology*, 100(7), e02720. Available from: <https://doi.org/10.1002/ecy.2720>

Chauvel, P.-A., Mussig, A.J., Hugenholtz, P. & Parks, D.H. (2019) GTDB-Tk: a toolkit to classify genomes with the genome taxonomy database. *Bioinformatics*, 36(6), 1925–1927. Available from: <https://doi.org/10.1093/bioinformatics/btz848>

Christensen, G.A., Gionfriddo, C.M., King, A.J., Moberly, J.G., Miller, C.L., Somenahally, A.C. et al. (2019) Determining the reliability of measuring mercury cycling gene abundance with correlations with mercury and methylmercury concentrations. *Environmental Science & Technology*, 53(15), 8649–8663. Available from: <https://doi.org/10.1021/acs.est.8b06389>

Christensen, G.A., Somenahally, A.C., Moberly, J.G., Miller, C.M., King, A.J., Gilmour, C.C. et al. (2018) Carbon amendments alter microbial community structure and net mercury methylation potential in sediments. *Applied and Environmental Microbiology*, 84(3), e01049–e01017. Available from: <https://doi.org/10.1128/AEM.01049-17>

Chu, C., Erickson, P.R., Lundein, R.A., Stamatelatos, D., Alaimo, P.J., Latch, D.E. et al. (2016) Photochemical and nonphotochemical transformations of cysteine with dissolved organic matter. *Environmental Science & Technology*, 50(12), 6363–6373. Available from: <https://doi.org/10.1021/acs.est.6b01291>

Cleckner, L.B., Gilmour, C.C., Hurley, J.P. & Krabbenhoft, D.P. (1999) Mercury methylation in periphyton of the Florida Everglades. *Limnology and Oceanography*, 44(7), 1815–1825. Available from: <https://doi.org/10.4319/lo.1999.44.7.1815>

Coleman Wasik, J.K., Engstrom, D.R., Mitchell, C.P.J., Swain, E.B., Monson, B.A., Balogh, S.J. et al. (2015) The effects of hydrologic fluctuation and sulfate regeneration on mercury cycling in an experimental peatland. *Journal of Geophysical Research: Biogeosciences*, 120, 1033–1047.

Biogeosciences, 120(9), 1697–1715. Available from: <https://doi.org/10.1002/2015JG002993>

Coleman Wasik, J.K., Mitchell, C.P.J., Engstrom, D.R., Swain, E.B., Monson, B.A., Balogh, S.J. et al. (2012) Methylmercury declines in a boreal peatland when experimental sulfate deposition decreases. *Environmental Science & Technology*, 46(12), 6663–6671. Available from: <https://doi.org/10.1021/es300865f>

Compeau, G.C. & Bartha, R. (1985) Sulfate-reducing bacteria: principal methylators of mercury in anoxic estuarine sediment. *Applied and Environmental Microbiology*, 50(2), 498–502.

DeWild, J.F., Olson, M.L. & Olund, S.D. (2002) Determination of methyl mercury by aqueous phase ethylation, followed by gas chromatographic separation with cold vapor atomic fluorescence detection. Open-file report (No. 2001–445). U. S. Geological Survey.

Eren, A.M., Esen, Ö.C., Quince, C., Vineis, J.H., Morrison, H.G., Sogin, M.L. et al. (2015) Anvio: an advanced analysis and visualization platform for omics data. *PeerJ*, 3, e1319. Available from: <https://doi.org/10.7717/peerj.1319>

Fu, L., Niu, B., Zhu, Z., Wu, S. & Li, W. (2012) CD-HIT: accelerated for clustering the next-generation sequencing data. *Bioinformatics*, 28(23), 3150–3152. Available from: <https://doi.org/10.1093/bioinformatics/bts565>

Gascón Diez, E., Loizeau, J.-L., Cosio, C., Bouchet, S., Adatte, T., Amouroux, D. et al. (2016) Role of settling particles on mercury methylation in the oxic water column of freshwater systems. *Environmental Science & Technology*, 50(21), 11672–11679. Available from: <https://doi.org/10.1021/acs.est.6b03260>

Gerbig, C.A., Kim, C.S., Stegemeier, J.P., Ryan, J.N. & Aiken, G.R. (2011) Formation of nanocolloidal metacinnabar in mercury-DOM-sulfide systems. *Environmental Science & Technology*, 45(21), 9180–9187. Available from: <https://doi.org/10.1021/es201837h>

Gilmour, C.C., Bullock, A.L., McBurney, A., Podar, M. & Elias, D.A. (2018) Robust mercury methylation across diverse methanogenic archaea. *mBio*, 9(2), 1–13. Available from: <https://doi.org/10.1128/mBio.02403-17>

Gilmour, C.C., Elias, D.A., Kucken, A.M., Brown, S.D., Palumbo, A.V., Schadt, C.W. et al. (2011) Sulfate-reducing bacterium *Desulfovibrio desulfuricans* ND132 as a model for understanding bacterial mercury methylation. *Applied and Environmental Microbiology*, 77(12), 3938–3951. Available from: <https://doi.org/10.1128/AEM.02993-10>

Gilmour, C.C., Henry, E.A. & Mitchell, R. (1992) Sulfate stimulation of mercury methylation in freshwater sediments. *Environmental Science & Technology*, 26(11), 2281–2287. Available from: <https://doi.org/10.1021/es00035a029>

Gilmour, C.C., Krabbenhoft, D., Orem, W.H., Aiken, G. & Roden, E. (2007) Appendix 3B-2: Status report on ACME studies on the control of mercury methylation and bioaccumulation in the Everglades. *South Florida Environmental Report, Volume I*, 3B-2-1 - 3B-2-39.

Gilmour, C.C., Podar, M., Bullock, A.L., Graham, A.M., Brown, S.D., Somenahally, A.C. et al. (2013) Mercury methylation by novel microorganisms from new environments. *Environmental Science & Technology*, 47(20), 11810–11820. Available from: <https://doi.org/10.1021/es403075t>

Gilmour, C.C., Riedel, G.S., Ederington, M.C., Bell, J.T., Benoit, J.M., Gill, G.A. et al. (1998) Methylmercury concentrations and production rates across a trophic gradient in the northern Everglades. *Biogeochemistry*, 40, 327–345. Available from: <https://doi.org/10.1023/A:1005972708616>

Gionfriddo, C.M., Capo, E., Peterson, B.D., Heyu, L., Jones, D.S., Bravo, A.G. et al. (2021) Hg-MATE-Db.v1.01142021. The Smithsonian Institution. <http://doi.org/10.25573/serc.13105370.v1>.

Gionfriddo, C.M., Tate, M.T., Wick, R.R., Schultz, M.B., Zemla, A., Thelen, M.P. et al. (2016) Microbial mercury methylation in Antarctic Sea ice. *Nature Microbiology*, 1(10), 16127. Available from: <https://doi.org/10.1038/nmicrobiol.2016.127>

Gionfriddo, C.M., Wymore, A.M., Jones, D.S., Wilpiszeski, R.L., Lynes, M.M., Christensen, G.A. et al. (2020) An improved *hgcAB* primer set and direct high-throughput sequencing expand Hg-methylator diversity in nature. *Frontiers in Microbiology*, 11, 1–23. Available from: <https://doi.org/10.3389/fmicb.2020.541554>

Goñi-Urriza, M., Corsellis, Y., Lancelier, L., Tessier, E., Gury, J., Monperrus, M. et al. (2015) Relationships between bacterial energetic metabolism, mercury methylation potential, and *hgcA/hgcB* gene expression in *Desulfovibrio desulfuroacetivorans* BerOct1. *Environmental Science and Pollution Research*, 22(18), 13764–13771. Available from: <https://doi.org/10.1007/s11356-015-4273-5>

Graham, A.M., Aiken, G.R. & Gilmour, C.C. (2012) Dissolved organic matter enhances microbial mercury methylation under sulfidic conditions. *Environmental Science & Technology*, 46(5), 2715–2723. Available from: <https://doi.org/10.1021/es203658f>

Graham, A.M., Aiken, G.R. & Gilmour, C.C. (2013) Effect of dissolved organic matter source and character on microbial Hg methylation in Hg–S–DOM solutions. *Environmental Science & Technology*, 47(11), 5746–5754. Available from: <https://doi.org/10.1021/es400414a>

Graham, A.M., Cameron-Burr, K.T., Hajic, H.A., Lee, C., Msekela, D. & Gilmour, C.C. (2017) Sulfurization of dissolved organic matter increases Hg–sulfide–dissolved organic matter bioavailability to a Hg-methylating bacterium. *Environmental Science & Technology*, 51(16), 9080–9088. Available from: <https://doi.org/10.1021/acs.est.7b02781>

Guimarães, J.R.D., Mauro, J.B.N., Meili, M., Sundbom, M., Haglund, A.L., Coelho-Souza, S.A. et al. (2006) Simultaneous radioassays of bacterial production and mercury methylation in the periphyton of a tropical and a temperate wetland. *Journal of Environmental Management*, 81(2), 95–100. Available from: <https://doi.org/10.1016/j.jenvman.2005.09.023>

Haitzer, M., Aiken, G.R. & Ryan, J.N. (2002) Binding of mercury(II) to dissolved organic matter: the role of the mercury-to-DOM concentration ratio. *Environmental Science & Technology*, 36(16), 3564–3570. Available from: <https://doi.org/10.1021/es025699i>

Hatzenpichler, R. (2020) Next-generation physiology approaches to study microbiome function at single cell level. *Nature Reviews Microbiology*, 18, 16–256. Available from: <https://doi.org/10.1038/s41579-020-0323-1>

Hinckley, E.-L.S., Crawford, J.T., Fakhraei, H. & Driscoll, C.T. (2020) A shift in sulfur-cycle manipulation from atmospheric emissions to agricultural additions. *Nature Geoscience*, 13(9), 597–604. Available from: <https://doi.org/10.1038/s41561-020-0620-3>

Hintemann, H. & Evans, R.D. (1997) Application of stable isotopes in environmental tracer studies—measurement of monomethylmercury (CH_3Hg^+) by isotope dilution ICP-MS and detection of species transformation. *Fresenius' Journal of Analytical Chemistry*, 358(3), 378–385. Available from: <https://doi.org/10.1007/s00160050433>

Hsu-Kim, H., Kucharzyk, K.H., Zhang, T. & Deshusses, M.A. (2013) Mechanisms regulating mercury bioavailability for methylating microorganisms in the aquatic environment: a critical review. *Environmental Science & Technology*, 47(6), 2441–2456. Available from: <https://doi.org/10.1021/es304370g>

Hurley, J.P., Krabbenhoft, D.P., Cleckner, L.B., Olson, M.L., Aiken, G.R. & Jr, P.S.R. (1998) System controls on the aqueous distribution of mercury in the northern Florida Everglades. *Biogeochemistry*, 40, 293–310. Available from: <https://doi.org/10.1023/A:1005928927272>

Hyatt, D., Chen, G.-L., LoCascio, P.F., Land, M.L., Larimer, F.W. & Hauser, L.J. (2010) Prodigal: prokaryotic gene recognition and translation initiation site identification. *BMC Bioinformatics*, 11(119), 1–11. Available from: <https://doi.org/10.1186/1471-2105-11-119>

Janssen, S.E., Schaefer, J.K., Barkay, T. & Reinfelder, J.R. (2016) Fractionation of mercury stable isotopes during microbial methyl-mercury production by iron- and sulfate-reducing bacteria. *Environmental Science & Technology*, 50(15), 8077–8083. Available from: <https://doi.org/10.1021/acs.est.6b00854>

Jones, D.S., Johnson, N.W., Mitchell, C.P.J., Walker, G.M., Bailey, J.V., Pastor, J. et al. (2020) Diverse communities of hgcAB⁺ microorganisms methylate mercury in freshwater sediments subjected to experimental sulfate loading. *Environmental Science & Technology*, 54, 14265–14274. Available from: <https://doi.org/10.1021/acs.est.0c02513>

Jones, D.S., Walker, G.M., Johnson, N.W., Mitchell, C.P.J., Coleman Wasik, J.K. & Bailey, J.V. (2019) Molecular evidence for novel mercury methylating microorganisms in sulfate-impacted lakes. *The ISME Journal*, 13, 1659–1675. Available from: <https://doi.org/10.1038/s41396-019-0376-1>

Jonsson, S., Skyllberg, U., Nilsson, M.B., Lundberg, E., Andersson, A. & Björn, E. (2014) Differentiated availability of geochemical mercury pools controls methylmercury levels in estuarine sediment and biota. *Nature Communications*, 5, 4624. Available from: <https://doi.org/10.1038/ncomms5624>

Jonsson, S., Skyllberg, U., Nilsson, M.B., Westlund, P.-O., Shchukarev, A., Lundberg, E. et al. (2012) Mercury methylation rates for geochemically relevant Hg^{II} species in sediments. *Environmental Science & Technology*, 46(21), 11653–11659. Available from: <https://doi.org/10.1021/es3015327>

Krabbenhoft, D.P., Hurley, J.P., Olson, M.L. & Cleckner, L.B. (1998) Diel variability of mercury phase and species distributions in the Florida Everglades. *Biogeochemistry*, 40, 311–325. Available from: <https://doi.org/10.1023/A:1005938607225>

Kucharzyk, K.H., Deshusses, M.A., Porter, K.A. & Hsu-Kim, H. (2015) Relative contributions of mercury bioavailability and microbial growth rate on net methylmercury production by anaerobic mixed cultures. *Environmental Science: Processes & Impacts*, 17(9), 1568–1577. Available from: <https://doi.org/10.1039/C5EM00174A>

Lever, M.A., Torti, A., Eickenbusch, P., Michaud, A.B., Šantl-Temkiv, T. & Jørgensen, B.B. (2015) A modular method for the extraction of DNA and RNA, and the separation of DNA pools from diverse environmental sample types. *Frontiers in Microbiology*, 6, 1–25. Available from: <https://doi.org/10.3389/fmicb.2015.00476>

Li, D., Liu, C.-M., Luo, R., Sadakane, K. & Lam, T.-W. (2015) MEGA-HIT: an ultra-fast single-node solution for large and complex metagenomics assembly via succinct de Bruijn graph. *Bioinformatics*, 31(10), 1674–1676. Available from: <https://doi.org/10.1093/bioinformatics/btv033>

Liu, Y.-R., Johs, A., Bi, L., Lu, X., Hu, H.-W., Sun, D. et al. (2018) Unraveling microbial communities associated with methylmercury production in paddy soils. *Environmental Science & Technology*, 52(22), 13110–13118. Available from: <https://doi.org/10.1021/acs.est.8b03052>

Luek, J.L., Thompson, K.E., Larsen, R.K., Heyes, A. & Gonsior, M. (2017) Sulfate reduction in sediments produces high levels of chromophoric dissolved organic matter. *Scientific Reports*, 7, 8829. Available from: <https://doi.org/10.1038/s41598-017-09223-z>

Manceau, A., Lemouchi, C., Rovezzi, M., Lanson, M., Glatzel, P., Nagy, K.L. et al. (2015) Structure, bonding, and stability of mercury complexes with thiolate and thioether ligands from high-resolution XANES spectroscopy and first-principles calculations. *Inorganic Chemistry*, 54(24), 11776–11791. Available from: <https://doi.org/10.1021/acs.inorgchem.5b01932>

Marvin-DiPasquale, M.C. & Orem, R.S. (1998) Bacterial methyl-mercury degradation in Florida Everglades peat sediment. *Environmental Science & Technology*, 32(17), 2556–2563. Available from: <https://doi.org/10.1021/es9710991>

McDaniel, E.A., Peterson, B.D., Stevens, S.L.R., Tran, P.Q., Anantharaman, K. & McMahon, K.D. (2020) Expanded phylogenetic diversity and metabolic flexibility of mercury-methylating microorganisms. *mSystems*, 5(4), 1–21. Available from: <https://doi.org/10.1128/mSystems.00299-20>

Millera Ferriz, L., Ponton, D.E., Storck, V., Leclerc, M., Bilodeau, F., Walsh, D.A. et al. (2021) Role of organic matter and microbial communities in mercury retention and methylation in sediments near run-of-river hydroelectric dams. *Science of the Total Environment*, 774, 145686. Available from: <https://doi.org/10.1016/j.scitotenv.2021.145686>

Mitchell, C.P.J., Branfireun, B.A. & Kolka, R.K. (2008) Assessing sulfate and carbon controls on net methylmercury production in peatlands: an in situ mesocosm approach. *Applied Geochemistry*, 23(3), 503–518. Available from: <https://doi.org/10.1016/j.apgeochem.2007.12.020>

Moreau, J.W., Gionfriddo, C.M., Krabbenhoft, D.P., Ogorek, J.M., DeWild, J.F., Aiken, G.R. et al. (2015) The effect of natural organic matter on mercury methylation by *Desulfovibrio propionicus* 1pr3. *Frontiers in Microbiology*, 6, 1389. Available from: <https://doi.org/10.3389/fmicb.2015.01389>

Munson, K.M., Lamborg, C.H., Boiteau, R.M. & Saito, M.A. (2018) Dynamic mercury methylation and demethylation in oligotrophic marine water. *Biogeosciences*, 15, 6451–6460. Available from: <https://doi.org/10.5194/bg-2018-173>

Newport, P.J. & Nedwell, D.B. (1988) The mechanisms of inhibition of *Desulfovibrio* and *Desulfotomaculum* species by selenate and molybdate. *Journal of Applied Bacteriology*, 65(5), 419–423. Available from: <https://doi.org/10.1111/j.1365-2672.1988.tb01911.x>

Nurk, S., Meleshko, D., Korobeynikov, A. & Pevzner, P.A. (2017) metaSPAdes: a new versatile metagenomic assembler. *Genome Research*, 27(5), 824–834. Available from: <https://doi.org/10.1101/gr.213959.116>

Olund, S.D., DeWild, J.F., Olson, M.L. & Tate, M.T. (2004) Chapter A8: Methods for the preparation and analysis of solids and suspended solids for total mercury. In: *U.S. Geological Survey techniques of water-resources investigations, Book 5*. Reston, VA: United States Geological Survey.

Orem, W.H., Gilmour, C., Axelrad, D., Krabbenhoft, D., Scheidt, D., Kalla, P. et al. (2011) Sulfur in the South Florida ecosystem: distribution, sources, biogeochemistry, impacts, and management for restoration. *Critical Reviews in Environmental Science and Technology*, 41, 249–288. Available from: <https://doi.org/10.1080/10643389.2010.531201>

Orem, W.H., Krabbenhoft, D.P., Poulin, B.A. & Aiken, G.R. (2020) Chapter 2: Sulfur contamination in the Everglades, a major control on mercury methylation. In: *Mercury and the Everglades. A synthesis and model for complex ecosystem restoration: Volume II – aquatic mercury cycling and bioaccumulation in the Everglades*. Switzerland: Springer International Publishing. Available from: <https://doi.org/10.1007/978-3-030-32057-7>

Parks, J.M., Johs, A., Podar, M., Bridou, R., Hurt, R.A., Smith, S.D. et al. (2013) The genetic basis for bacterial mercury methylation. *Science*, 339(6125), 1332–1335. Available from: <https://doi.org/10.1126/science.1230667>

Peterson, B.D., McDaniel, E.A., Schmidt, A.G., Lepak, R.F., Janssen, S.E., Tran, P.Q. et al. (2020) Mercury methylation genes identified across diverse anaerobic microbial guilds in a eutrophic sulfate-enriched lake. *Environmental Science & Technology*, 54, 15840–15851. Available from: <https://doi.org/10.1021/acs.est.0c05435>

Podar, M., Gilmour, C.C., Brandt, C.C., Soren, A., Brown, S.D., Crable, B.R. et al. (2015) Global prevalence and distribution of genes and microorganisms involved in mercury methylation. *Science Advances*, 1(9), e1500675. Available from: <https://doi.org/10.1126/sciadv.1500675>

Poulin, B.A., Gerbig, C.A., Kim, C.S., Stegemeier, J.P., Ryan, J.N. & Aiken, G.R. (2017) Effects of sulfide concentration and dissolved

organic matter characteristics on the structure of nanocolloidal metacinnabar. *Environmental Science & Technology*, 51(22), 13133–13142. Available from: <https://doi.org/10.1021/acs.est.7b02687>

Poulin, B.A., Ryan, J.N., Nagy, K.L., Stubbins, A., Dittmar, T., Orem, W.H. et al. (2017) Spatial dependence of reduced sulfur in Everglades dissolved organic matter controlled by sulfate enrichment. *Environmental Science & Technology*, 51(7), 3630–3639. Available from: <https://doi.org/10.1021/acs.est.6b04142>

Poulin, B.A., Ryan, J.N., Tate, M.T., Krabbenhoft, D.P., Hines, M.E., Barkay, T. et al. (2019) Geochemical factors controlling dissolved elemental mercury and methylmercury formation in Alaskan wetlands of varying trophic status. *Environmental Science & Technology*, 53(11), 6203–6213. Available from: <https://doi.org/10.1021/acs.est.8b06041>

Roth, S., Poulin, B.A., Baumann, Z., Liu, X., Zhang, L., Krabbenhoft, D.P. et al. (2021) Nutrient inputs stimulate mercury methylation by syntrophs in a subarctic peatland. *Frontiers in Microbiology*, 12, 1–14. Available from: <https://doi.org/10.3389/fmicb.2021.741523>

Schaefer, J.K., Kronberg, R., Björn, E. & Skjellberg, U. (2020) Anaerobic guilds responsible for mercury methylation in boreal wetlands of varied trophic status serving as either a methylmercury source or sink. *Environmental Microbiology*, 22(9), 3685–3699. Available from: <https://doi.org/10.1111/1462-2920.15134>

Schaefer, J.K. & Morel, F.M.M. (2009) High methylation rates of mercury bound to cysteine by *Geobacter sulfurreducens*. *Nature Geoscience*, 2(2), 123–126. Available from: <https://doi.org/10.1038/ngeo412>

Schaefer, J.K., Rocks, S.S., Zheng, W., Liang, L., Gu, B. & Morel, F. M.M. (2011) Active transport, substrate specificity, and methylation of Hg(II) in anaerobic bacteria. *Proceedings of the National Academy of Sciences*, 108(21), 8714–8719. Available from: <https://doi.org/10.1073/pnas.1105781108>

Sieber, J.R., McInerney, M.J. & Gunsalus, R.P. (2012) Genomic insights into syntrophy: the paradigm for anaerobic metabolic cooperation. *Annual Review of Microbiology*, 66(1), 429–452. Available from: <https://doi.org/10.1146/annurev-micro-090110-102844>

Smith, S.D., Bridou, R., Johs, A., Parks, J.M., Elias, D.A., Hurt, R.A. et al. (2015) Site-directed mutagenesis of *hgcA* and *hgcB* reveals amino acid residues important for mercury methylation. *Applied and Environmental Microbiology*, 81(9), 3205–3217. Available from: <https://doi.org/10.1128/AEM.00217-15>

Sorek, R., Zhu, Y., Creevey, C.J., Francino, M.P., Bork, P. & Rubin, E.M. (2007) Genome-wide experimental determination of barriers to horizontal gene transfer. *Science*, 318(5855), 1449–1452. Available from: <https://doi.org/10.1126/science.1147112>

Stamatakis, A. (2014) RAxML version 8: a tool for phylogenetic analysis and post-analysis of large phylogenies. *Bioinformatics*, 30(9), 1312–1313. Available from: <https://doi.org/10.1093/bioinformatics/btu033>

Tada, Y., Marumoto, K. & Takeuchi, A. (2020) Nitrospina-like bacteria are potential mercury methylators in the mesopelagic zone in the East China Sea. *Frontiers in Microbiology*, 11, 1369. Available from: <https://doi.org/10.3389/fmicb.2020.01369>

Tate, M.T., DeWild, J.F., Ogorek, J.M., Janssen, S.E., Krabbenhoft, D.P., Poulin, B.A. et al. (2023) Chemical characterization of water, sediments, and fish from Water Conservation Areas and Canals of the Florida Everglades (USA), 2012 to 2019 (U.S. Geological Survey data release). <http://10.5066/P976EGIX>

Tjerngren, I., Karlsson, T., Björn, E. & Skjellberg, U. (2012) Potential Hg methylation and MeHg demethylation rates related to the nutrient status of different boreal wetlands. *Biogeochemistry*, 108(1–3), 335–350. Available from: <https://doi.org/10.1007/s10533-011-9603-1>

Vairavamurthy, A. & Mopper, K. (1987) Geochemical formation of organosulphur compounds (thiols) by addition of H₂S to sedimentary organic matter. *Nature*, 329(6140), 623–625. Available from: <https://doi.org/10.1038/329623a0>

Wiener, J.G., Krabbenhoft, D.P., Heinz, G.H. & Scheuhammer, A.M. (2003) Chapter 16: Ecotoxicology of mercury. In: Hoffman, D.J., Rattner, B.A., Burton, G.A. & Cairns, J. (Eds.) *Handbook of Ecotoxicology*, 2nd edition. Boca Raton, FL: CRC Press, pp. 407–461.

Yu, R.-Q., Reinfelder, J.R., Hines, M.E. & Barkay, T. (2018) Syntrophic pathways for microbial mercury methylation. *The ISME Journal*, 12(7), 1826–1835. Available from: <https://doi.org/10.1038/s41396-018-0106-0>

Zhang, J., Wang, F., House, J.D. & Page, B. (2004) Thiols in wetland interstitial waters and their role in mercury and methylmercury speciation. *Limnology and Oceanography*, 49(6), 2276–2286. Available from: <https://doi.org/10.4319/lo.2004.49.6.2276>

Zhang, T., Kim, B., Levard, C., Reinsch, B.C., Lowry, G.V., Deshusses, M.A. et al. (2012) Methylation of mercury by bacteria exposed to dissolved, nanoparticulate, and microparticulate mercuric sulfides. *Environmental Science & Technology*, 46(13), 6950–6958. Available from: <https://doi.org/10.1021/es203181m>

Zhou, Z., Tran, P.Q., Breister, A.M., Liu, Y., Kieft, K., Cowley, E.S. et al. (2022) METABOLIC: high-throughput profiling of microbial genomes for functional traits, metabolism, biogeochemistry, and community-scale functional networks. *Microbiome*, 10(33), 1–22. Available from: <https://doi.org/10.1186/s40168-021-01213-8>

SUPPORTING INFORMATION

Additional supporting information can be found online in the Supporting Information section at the end of this article.

How to cite this article: Peterson, B.D., Krabbenhoft, D.P., McMahon, K.D., Ogorek, J.M., Tate, M.T., Orem, W.H. et al. (2023) Environmental formation of methylmercury is controlled by synergy of inorganic mercury bioavailability and microbial mercury-methylation capacity. *Environmental Microbiology*, 25(8), 1409–1423. Available from: <https://doi.org/10.1111/1462-2920.16364>